



Cell Identity Mediates the Response of *Arabidopsis* Roots to Abiotic Stress

José R. Dinneny *et al.*
Science **320**, 942 (2008);
 DOI: 10.1126/science.1153795

This copy is for your personal, non-commercial use only.

If you wish to distribute this article to others, you can order high-quality copies for your colleagues, clients, or customers by [clicking here](#).

Permission to republish or repurpose articles or portions of articles can be obtained by following the guidelines [here](#).

The following resources related to this article are available online at www.sciencemag.org (this information is current as of September 18, 2012):

A correction has been published for this article at:
<http://www.sciencemag.org/content/322/5898/44.2.full.html>

Updated information and services, including high-resolution figures, can be found in the online version of this article at:
<http://www.sciencemag.org/content/320/5878/942.full.html>

Supporting Online Material can be found at:
<http://www.sciencemag.org/content/suppl/2008/10/02/320.5878.942.DC1.html>

A list of selected additional articles on the Science Web sites **related to this article** can be found at:
<http://www.sciencemag.org/content/320/5878/942.full.html#related>

This article has been **cited by** 50 article(s) on the ISI Web of Science

This article has been **cited by** 49 articles hosted by HighWire Press; see:
<http://www.sciencemag.org/content/320/5878/942.full.html#related-urls>

This article appears in the following **subject collections**:
 Botany
<http://www.sciencemag.org/cgi/collection/botany>

Cell Identity Mediates the Response of *Arabidopsis* Roots to Abiotic Stress

José R. Dinneny,^{1*†} Terri A. Long,^{1*} Jean Y. Wang,¹ Jee W. Jung,¹ Daniel Mace,² Solomon Pointer,¹ Christa Barron,³ Siobhan M. Brady,¹ John Schiefelbein,³ Philip N. Benfey^{1,2‡}

Little is known about the way developmental cues affect how cells interpret their environment. We characterized the transcriptional response to high salinity of different cell layers and developmental stages of the *Arabidopsis* root and found that transcriptional responses are highly constrained by developmental parameters. These transcriptional changes lead to the differential regulation of specific biological functions in subsets of cell layers, several of which correspond to observable physiological changes. We showed that known stress pathways primarily control semiubiquitous responses and used mutants that disrupt epidermal patterning to reveal cell-layer-specific and inter-cell-layer effects. By performing a similar analysis using iron deprivation, we identified common cell-type-specific stress responses and revealed the crucial role the environment plays in defining the transcriptional outcome of cell-fate decisions.

High salinity is an important agricultural contaminant (1) and has complex effects on root physiology. Although a small set of studies has begun to explore salt responses at the cell-type-specific level (2, 3), it remains unclear to what extent cell identity influences stress responses and what mechanisms enable this regulation. To directly address these issues, we generated a genome-scale, high-resolution expression map for roots grown under standard and high-salinity conditions (4). We first performed a phenotypic analysis using different concentrations of salt and a time-course analysis [TC data set in the supporting online material (SOM) text, Fig. 1, A and F, fig. S1, and tables S1 and S2] of the response of whole roots to salt to select the specific parameters (1 hour of exposure to 140 mM NaCl) for our spatial microarray analysis.

The root of *Arabidopsis* grows from stem cells at the tip. We dissected roots into four longitudinal zones (LZ data set in Fig. 1A and table S1) for analysis, using the position of cells along the longitudinal axis as a proxy for developmental time (fig. S2) (5). Cell identity varies along the radial axis; epidermal cells constitute the outermost tissue, followed by the cortex, endodermis, and the central stele (fig. S2). Cell-type-specific transcriptional profiles were generated by fluorescence-activated cell sorting (FACS) of roots that express green fluorescent protein (GFP) reporters in specific cell types (6, 7) (RZ data set in Fig. 1A and table S1). Six different GFP reporters were used to profile all radial zones, including the columella root cap and phloem vasculature (fig. S3 and table S3). Intact roots rather than protoplasted or

isolated populations of cells were exposed to salt to ensure that the observed transcriptional response occurred in the context of the whole

organ. We performed control experiments to test the effects of sorting on salt-responsive genes (SOM text and tables S4 and S5) and used GFP reporters (8) along with image analysis software (9) to validate the accuracy of the RZ microarray data (Fig. 1, B to D, and figs. S4 and S5).

With stringent statistical significance criteria, we identified increasing numbers of differentially expressed genes at higher spatial resolution: 238 (at 1 hour), 1173, and 3862 genes were identified in our TC, LZ, and RZ experiments, respectively (Fig. 1A and table S2). Genes regulated in our TC experiment tended to respond to salt stress in multiple radial or longitudinal zones, whereas the majority of genes regulated in the spatial data sets changed in only one zone (Fig. 1, E, G, and H, and fig. S6).

One explanation for the prevalence of cell-type-specific responses may be that salt might not have fully penetrated all root tissues, which led to localized responses. We found, however, that internal tissues tend to be highly responsive; 48% of salt-responsive genes were regulated in

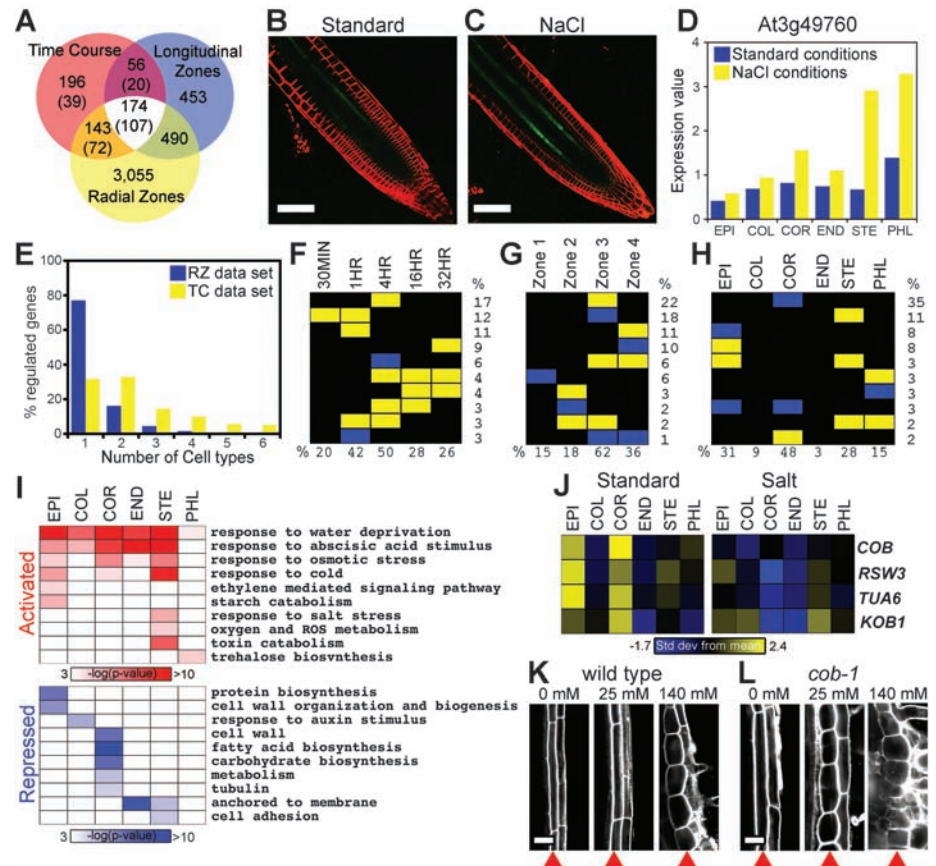


Fig. 1. Salt-stress microarray data sets. (A) Venn diagram showing overlap between data sets (1-hour TC comparisons in parentheses). (B to D) Salt-responsive GFP-reporter [(B) and (C)] for At3g49760 and associated microarray data (D). EPI, epidermis and lateral root cap; COL, columella root cap; COR, cortex; END, endodermis and quiescent center; STE, stele; PHL, protophloem. (E) Percentage of genes regulated in one to six cell types identified in the TC and RZ data sets, respectively. (F to H) Ten most common transcriptional changes in each data set and percent of responsive genes in each experiment (bottom row). Yellow indicates up-regulated genes; blue indicates down-regulated genes. (I) Enriched Gene-Ontology categories. (J) Expression patterns for cell-shape regulators in response to salt. (K and L) Cortex cells (arrowheads) swell in response to salt. *cob-1* mutants are hypersensitive to NaCl. Scale bars indicate 50 μ m [(B) and (C)] and 30 μ m [(K) and (L)].

¹Department of Biology, Duke University, Durham, NC 27708, USA. ²Institute for Genome Sciences and Policy Center for Systems Biology, Duke University, Durham, NC 27708, USA. ³Department of Molecular, Cellular, and Developmental Biology, University of Michigan, Ann Arbor, MI 48109, USA.

*These authors contributed equally to this work.

†Present address: Temasek Lifesciences Laboratory, National University of Singapore, Singapore 117604, Singapore.

‡To whom correspondence should be addressed. E-mail: philip.benfey@duke.edu

the cortex (Fig. 1H), and similar numbers were regulated in the stele (28%) and in the epidermis (31%). Along the longitudinal axis, an increase in salt responsiveness correlates with the beginning of the elongation zone, in which cells begin to acquire their final shape and function (Fig. 1G).

Testing our LZ and RZ data sets for enrichment in Gene-Ontology (10) annotations (Fig. 1I, fig. S7, and tables S6 and S7), we found 50 to 82%, respectively, of enriched categories are zone-specific (fig. S8), indicating that salt stress regulates distinct processes on the basis of developmental

context. Categories associated with stresses, including abscisic acid (ABA) response, tend to be enriched in multiple cell types, suggesting that most previously characterized stress-response genes are not cell-type-specific.

Salt stress results in radial swelling of the outer tissue layers of roots (Fig. 1K and fig. S9) (11), resembling plants with mutations in genes important for cell-wall biogenesis or with reduced tubulin expression. Several of these genes are repressed in the cortex and epidermis, including *COBRA* (*COB*) (12), *RADIAL SWELLING3* (*RSW3*) (13), *TUBULIN ALPHA-6* (*TUA6*) (14),

and *KOBITO1* (*KOB1*) (15) (Fig. 1J). Gene-Ontology categories associated with these functions are also enriched (Fig. 1I). Consistent with these findings, a hypomorphic allele of *COB* enhances the salt-regulated radial swelling of the cortex, indicating that the expression changes facilitate the cell-shape changes (Fig. 1, K and L, and fig. S9).

We compared cis-element enrichment in the promoters of genes regulated in a zone-specific manner with genes regulated in at least three zones (semiubiquitous responders) for the LZ and RZ data sets, respectively (Fig. 2A and table S8). In the LZ data set, enrichment of many known cis elements, such as drought-responsive element (DRE) (16) and ABA-responsive element (ABRE) (17, 18), was observed in both gene sets, whereas enrichment was largely limited to the semiubiquitous gene set in the RZ data set. Thus, although canonical stress-response pathways appear to be active in all cell layers, cell-type-specific responses are distinguishable at the promoter level and probably controlled by other cis elements. This suggests that cell-type-specific salt responses are not simply controlled by a combination of stress- and developmental-regulatory elements in a single promoter.

The plant hormone ABA is known to mediate stress responses, and ABA-response mutants are partly resistant to high salinity (19). Strong enrichment of ABRE cis elements in the promoters of semiubiquitous responders suggested that ABA activity is present throughout the root. To test this, we examined the salt responsiveness of hormone-marker genes (20). We find enrichment of up-regulated ABA-marker genes in all cell layers of the root (Fig. 2B and table S9) and not for other hormones (fig. S10B). This apparent widespread activity suggested that ABA might primarily mediate semiubiquitous transcriptional responses to salt. We therefore monitored the effects of ABA deficiency on the expression of a set of cell-type-specific, salt-stress-activated genes (21, 22). We find that salt-induced expression is diminished for many of these genes, similar to a collection of semiubiquitous responders also tested (Fig. 2, C and D). Together, these results indicate that ABA regulates cell-type-specific responses to salt stress in a manner independent of characterized ABRE elements.

DRE and its derivatives are bound by a subclass of APETALA2 (AP2)- and ethylene-responsive element-binding protein-type transcription factors, such as *DREB2A* (23, 24). Strong DRE enrichment is detected in genes up-regulated in at least three radial zones (Fig. 2A). Consistent with this, *DREB2A* is expressed in all cell layers under salt-stress conditions (fig. S10C). Recently, potential direct targets of *DREB2A* have been identified (25). These targets tend to be up-regulated by salt in at least three cell types at a higher frequency than expected ($P = 6.5 \times 10^{-6}$, Fig. 2E, and table S10), supporting the hypothesis that the DRE/DREB2A regulatory module primarily controls semiubiquitous responses.

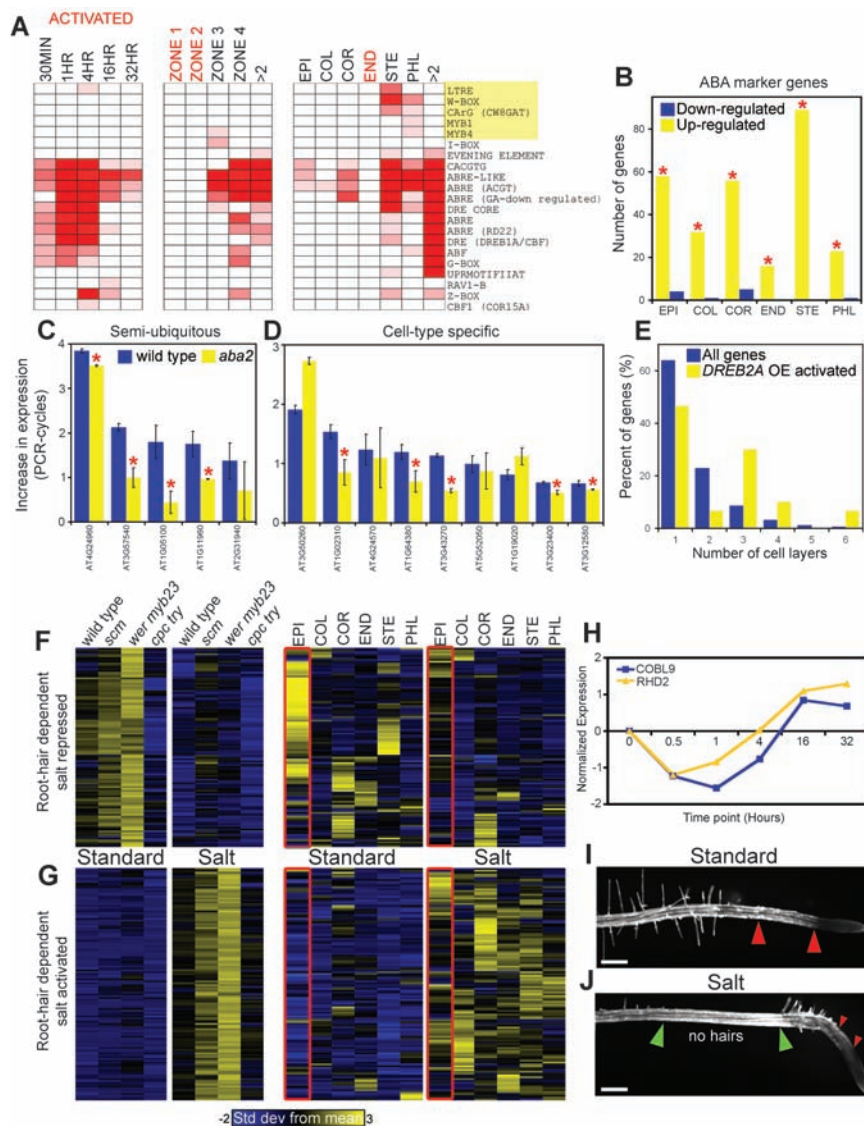


Fig. 2. Regulation of salt responses. (A) Enriched known cis-elements. Gene sets in red contain fewer than 50 genes. Shading indicates increasing statistical significance from $P = 1 \times 10^{-3}$ to $P = 1 \times 10^{-10}$; yellow box indicates cell-type-specific enriched cis elements. Figure S10A shows cis elements enriched in salt-repressed gene sets. (B) ABA-marker genes are up-regulated and enriched (asterisks, $P < 1 \times 10^{-4}$) in all cell layers. (C and D) The *aba-2* mutation significantly affects semiubiquitous and cell-type-specific salt-responsive genes (asterisks, $P < 0.05$). (E) *DREB2A* overexpression (OE) targets tend to be regulated in multiple cell types by salt. (F and G) Gene sets regulated by epidermal patterning and salt stress. (H) Hair-cell regulators are dynamically expressed in response to salt. (I and J) Hair-cell outgrowth is transiently suppressed by salt stress. Scale bars, 100 μm [(I) and (J)].

To understand how developmental pathways regulate salt responses, we transcriptionally profiled three mutants that alter cell-fate decisions in the epidermis: *werewolf myb23*, *caprice triptychon* (26), and *scrambled* (27) (fig. S11, A to D, and table S11). By using less-stringent significance criteria to aid in the identification of cell-type-specific responses, we identified four sets of genes whose activation or repression by salt is dependent on correct epidermal patterning (Fig. 2, F and G, fig. S11, F and G, and table S12). One gene set whose expression is hair-identity-dependent and repressed by salt shows enriched epidermal expression in the RZ data set under standard conditions, indicating that these genes are likely to be hair-cell-specific and salt-responsive (Fig. 2F). Root-hair elongation is inhibited by salt stress (28), and we find that many of these repressed genes encode structural components of the cell wall ($P = 1 \times 10^{-8}$) or are involved in trichoblast (hair-cell precursor) differentiation ($P = 1 \times 10^{-4}$). Several of these genes, such as *COBL9* (29) and *ROOT HAIR DEFECTIVE2 (RHD2)* (30), show fluctuating expression in the TC data set (Fig. 2H). By quantifying trichoblast cells that failed to form hairs, we were able to track the effects of salt stress on hair development. Hair outgrowth was initially suppressed by salt stress, then resumed after 8 hours of treatment (Fig. 2, I and J, and fig. S11E). Thus, the response of roots is not static but changes over time, potentially as a result of adaptation.

Unexpectedly, 51% of the genes whose expression is affected by salt and epidermal patterning are exclusively regulated in nonepidermal cell types, based on the RZ data set (table S12). Thus, cell-fate decisions may have nonautonomous effects on responses in other cell layers. We also identified 47 genes that respond most dramatically in hairless *caprice triptychon* mutants, indicating that a component of the variation in response is a direct outcome of changes in cell identity and not solely the effects of enhanced salt absorption in genetic backgrounds that develop hairs (fig. S11, F and G, and table S12).

To determine whether the trends we observed for salt stress hold for other environmental stimuli, we generated TC, LZ, and RZ data sets for roots exposed to iron-deficient media (-Fe, tables S1 and S2; control experiments described in SOM). On the basis of the TC data, we performed the LZ and RZ profiling at 24 hours. Iron is a necessary micronutrient and is used in diverse processes from photosynthesis to metabolism. Similar to the salt stress data set, increasing numbers of differentially expressed genes were detected with increasing spatial resolution [at 24 hours: TC, 111 genes; LZ, 142 genes; and RZ, 1318 genes] (Fig. 3A). Most genes are regulated in a zone-specific manner (Fig. 3, B to D, and fig. S12, A and B). Unlike salt stress, iron deprivation elicited the strongest transcriptional response after 24 hours of treatment in LZ 4 (85%) and in the stele (36%), where iron is predominantly stored in seeds and circulated in adult plants (31)

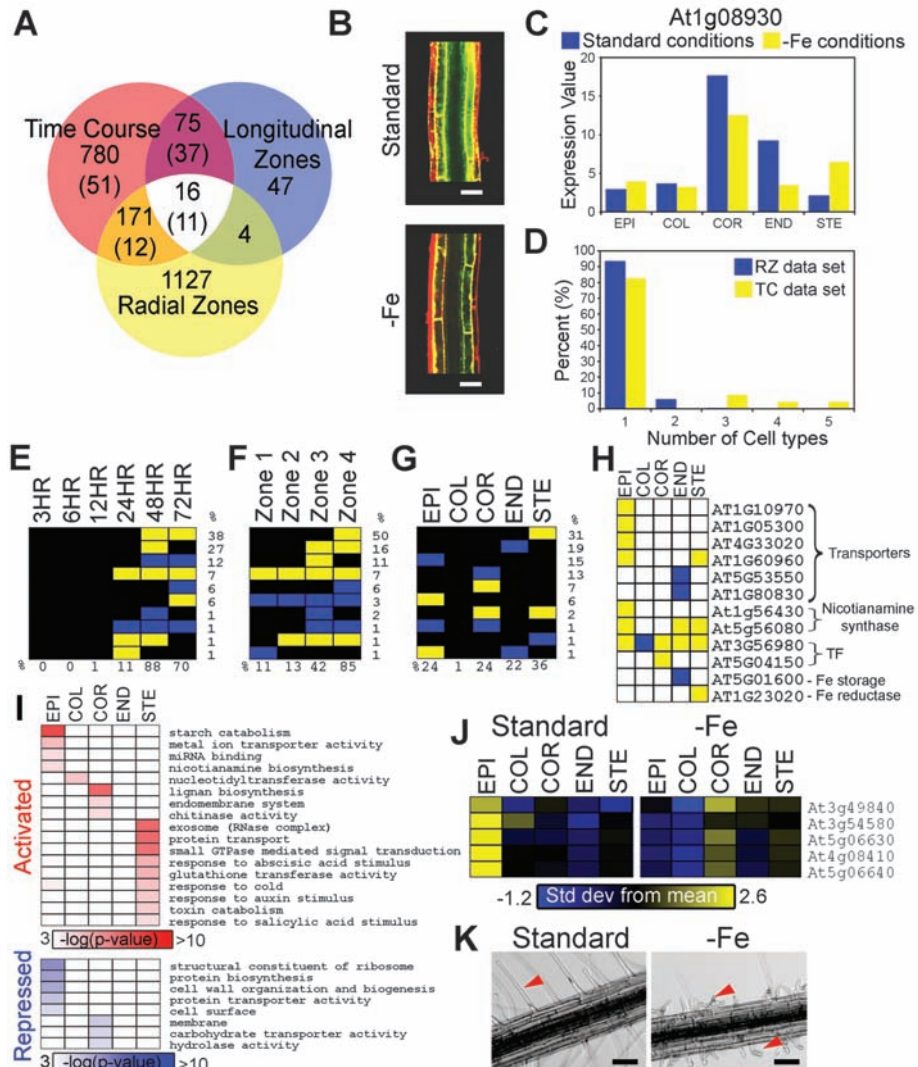


Fig. 3. Iron-deficiency microarray data sets. (A) Venn diagram showing overlap between data sets (1-hour TC comparisons in parentheses). (B) Iron-deficiency responsive GFP reporter (*At1g08930*) and associated microarray data (C). (D) Percentage of genes regulated in one to six cell types identified in the TC and RZ data sets, respectively. (E to G) Ten most common transcriptional changes in each data set and percent of the total responsive genes in each experiment (bottom row). Yellow indicates up-regulated genes; blue indicates down-regulated genes. (H) Regulation of putative and known iron-deprivation response genes. Yellow indicates up-regulated genes; blue indicates down-regulated genes (*At5g53550*, $FDR = 2.7 \times 10^{-5}$). (I) Enriched Gene-Ontology categories. miRNA, microRNA; RNase, ribonuclease; GTPase, guanosine triphosphatase. (J) Expression patterns for cell-wall biogenesis genes in response to iron deprivation (*At3g49840*, *At3g54580*, *At4g08410*, *At5g06630*, and *At5g06640*). (K) Root hairs are shorter and misshapen (arrows) in response to iron deprivation. Scale bars, 50 μm [(B) and (K)].

(Fig. 3, E to G, and fig. S12D). Putative and known genes encoding iron transporter, chelator, storage, metabolic, and regulatory proteins responded in a cell-type-specific manner (Fig. 3H and table S18) (32, 33). The stele response was enriched for generalized stress-responsive genes and suggests that iron deficiency may be sensed internally (Fig. 3I). Consistent with known roles in nutrient absorption, genes activated in the epidermis were enriched for metal-ion transport and nicotianamine (metal chelator) biosynthesis (Fig. 3I, fig. S12A, and table S7). Additionally, cell-wall biogenesis and organization

genes, such as the proline-rich extensins associated with root-hair morphogenesis (29), were down-regulated in epidermal cells and may explain the observed changes in root-hair morphology (Fig. 3, J and K) (34).

A comparison of the two RZ data sets revealed that 20% of salt-responsive genes also responded to iron deprivation (Fig. 4B and table S15). Of these, about half are scored with similar transcriptional changes across all five cell types (Fig. 4A). We initially hypothesized that semi-ubiquitous salt-responsive genes would be most likely to encompass a general stress response;

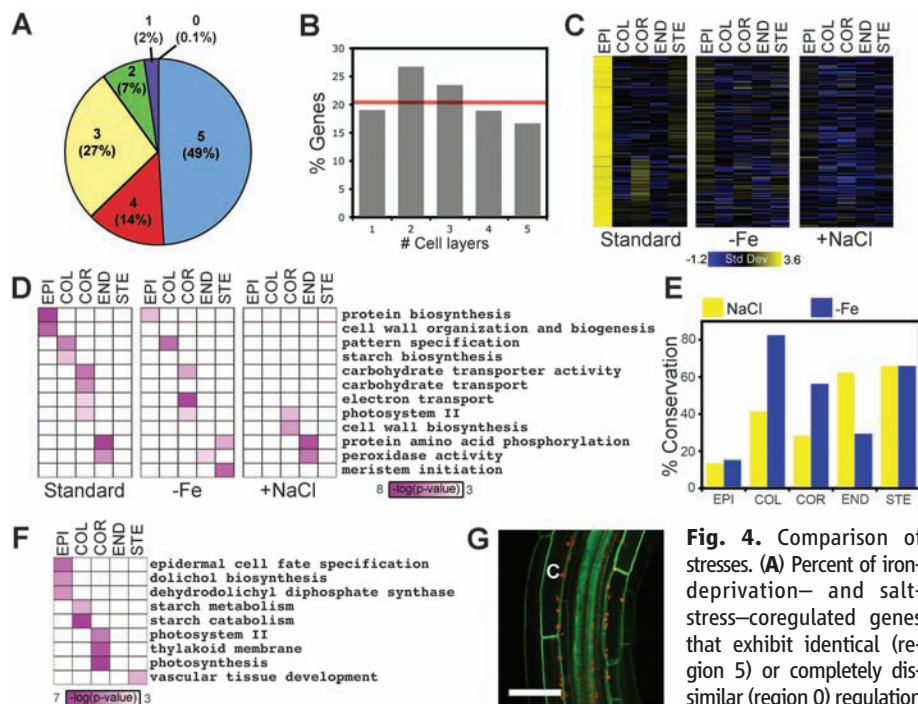


Fig. 4. Comparison of stresses. (A) Percent of iron-deprivation- and salt-stress-core-regulated genes that exhibit identical (region 5) or completely dissimilar (region 0) regulation in the RZ data set. (B) Percent of salt-stress-responsive genes that are also iron-deprivation responsive and the number of cell layers in which those genes respond under salt stress. Overall overlap is 20% (red line). (C) Super cluster (no. 406). Figure S13 lists other super clusters. (D) Gene-Ontology categories enriched in gene sets with environment-dependent cell-type-specific expression. (E) Percent conservation of cell-type-specific gene sets comparing standard conditions with stress gene sets, respectively. (F) Gene-Ontology categories enriched in gene sets with environment-independent cell-type-specific expression. (G) Chloroplast enrichment in the cortex (c). Chloroplasts also accumulate in the pericycle, which was not specifically profiled in these experiments. Scale bar, 50 μ m.

cent of salt-stress-responsive genes that are also iron-deprivation responsive and the number of cell layers in which those genes respond under salt stress. Overall overlap is 20% (red line). (C) Super cluster (no. 406). Figure S13 lists other super clusters. (D) Gene-Ontology categories enriched in gene sets with environment-dependent cell-type-specific expression. (E) Percent conservation of cell-type-specific gene sets comparing standard conditions with stress gene sets, respectively. (F) Gene-Ontology categories enriched in gene sets with environment-independent cell-type-specific expression. (G) Chloroplast enrichment in the cortex (c). Chloroplasts also accumulate in the pericycle, which was not specifically profiled in these experiments. Scale bar, 50 μ m.

however, genes responsive to salt in all five layers are the least likely to be coregulated by iron deprivation, indicating greater environmental specificity for these genes (Fig. 4B). This suggests that cell-type-specific biological processes are common targets for stress regulation, whereas responses occurring in all cells must be finely tuned for specific stimuli. To better understand shared responses, we used the Affinity-Propagation clustering algorithm (35) to identify gene sets that clustered in the iron-deprivation and salt-stress data sets (super clusters, table S15). The largest set of coregulated genes displayed concerted down-regulation in the epidermis and encoded genes important for protein biosynthesis (Fig. 4C and fig. S13A). Both stresses result in reduced root length (figs. S1, A to C, and S12C); this super cluster may represent a common stress module associated with growth suppression.

Previously we have shown that under standard conditions, many biological functions are regulated in a cell-type-specific manner (6, 36). On comparison of expression under standard conditions with these two stresses, we find that only 15% of cell-type-specific biological functions enriched under standard conditions are conserved (Fig. 4D, fig. S13, E and F, and table S16). Thus, the majority of a cell type's unique physiology is environment-dependent. Although the percent of

genes that exhibited stable expression patterns between standard conditions and each stress varied for most cell types, the epidermis consistently showed the least conservation (13 to 15%) (Fig. 4E). This trend holds despite the epidermis not being the most responsive cell type for either stress and suggests the functions that define this layer are particularly dependent on environmental constraints.

We identified 244 genes that are cell-type-specific and whose expression pattern does not substantially change with either stress (table S16). Enriched Gene-Ontology categories are consistent with known functions, and we discovered chloroplast accumulation as a novel feature of the cortex in light-grown roots (Fig. 4, F and G). Additionally, this gene set is enriched for many known regulators of cell identity (table S17), suggesting that a small set of core regulators maintain cell identity independent of environmental fluctuations.

Our results reveal that the transcriptional state of a cell is largely a reaction to environmental conditions that are regulated by a smaller core set of genes that stably determines cell identity. The use of environmental stimuli combined with cell- and developmental-stage-specific profiling will enable the identification of high-confidence transcriptional modules, an important first step in modeling transcriptional networks in multicellular organisms.

References and Notes

1. T. J. Flowers, A. Garcia, M. Koyama, A. R. Yeo, *Acta Physiol. Plant.* **19**, 427 (1997).
2. E. Kiegle, C. A. Moore, J. Haseloff, M. A. Tester, M. R. Knight, *Plant J.* **23**, 267 (2000).
3. S. Ma, H. J. Bohnert, *Genome Biol.* **8**, R49 (2007).
4. Material and methods are available on Science Online.
5. B. Scheres, P. Benfey, L. Dolan, in *The Arabidopsis Book*, C. R. Somerville, E. M. Meyerowitz, Eds. (American Society of Plant Biologists, Rockville, MD, 2002), pp. 1–18.
6. K. Birnbaum *et al.*, *Science* **302**, 1956 (2003).
7. K. Birnbaum *et al.*, *Nat. Methods* **2**, 615 (2005).
8. J. Y. Lee *et al.*, *Proc. Natl. Acad. Sci. U.S.A.* **103**, 6055 (2006).
9. D. L. Mace *et al.*, *Bioinformatics* **22**, e323 (2006).
10. M. Ashburner *et al.*, *Nat. Genet.* **25**, 25 (2000).
11. S. Burssens *et al.*, *Planta* **211**, 632 (2000).
12. G. Schindelman *et al.*, *Genes Dev.* **15**, 1115 (2001).
13. J. E. Burn *et al.*, *Plant J.* **32**, 949 (2002).
14. Y. Bao, B. Kost, N. H. Chua, *Plant J.* **28**, 145 (2001).
15. S. Pagant *et al.*, *Plant Cell* **14**, 2001 (2002).
16. K. Yamaguchi-Shinozaki, K. Shinozaki, *Plant Cell* **6**, 251 (1994).
17. J. Mundy, K. Yamaguchi-Shinozaki, N. H. Chua, *Proc. Natl. Acad. Sci. U.S.A.* **87**, 1406 (1990).
18. W. R. Marcotte Jr., S. H. Russell, R. S. Quatrano, *Plant Cell* **1**, 969 (1989).
19. P. Achard *et al.*, *Science* **311**, 91 (2006).
20. J. L. Nemhauser, F. Hong, J. Chory, *Cell* **126**, 467 (2006).
21. M. Gonzalez-Guzman *et al.*, *Plant Cell* **14**, 1833 (2002).
22. E. Nambara, H. Kawaide, Y. Kamiya, S. Naito, *Plant Cell Physiol.* **39**, 853 (1998).
23. Q. Liu *et al.*, *Plant Cell* **10**, 1391 (1998).
24. Y. Sakuma *et al.*, *Plant Cell* **18**, 1292 (2006).
25. Y. Sakuma *et al.*, *Proc. Natl. Acad. Sci. U.S.A.* **103**, 18822 (2006).
26. S. Schellmann *et al.*, *EMBO J.* **21**, 5036 (2002).
27. S. H. Kwak, R. Shen, J. Schiefelbein, *Science* **307**, 1111 (2005).
28. S. J. Halperin, S. Gilroy, J. P. Lynch, *J. Exp. Bot.* **54**, 1269 (2003).
29. M. A. Jones, M. J. Raymond, N. Smirnov, *Plant J.* **45**, 83 (2006).
30. J. Foreman *et al.*, *Nature* **422**, 442 (2003).
31. S. A. Kim *et al.*, *Science* **314**, 1295 (2006).
32. S. A. Kim, M. L. Gueriot, *FEBS Lett.* **581**, 2273 (2007).
33. H. Y. Wang *et al.*, *Planta* **226**, 897 (2007).
34. M. Muller, W. Schmidt, *Plant Physiol.* **134**, 409 (2004).
35. B. J. Frey, D. Dueck, *Science* **315**, 972 (2007).
36. S. M. Brady *et al.*, *Science* **318**, 801 (2007).
37. We thank D. Orlando for writing the R-script used for running the affinity propagation clustering algorithm; A. Pillai, D. McClay, D. Sherwood, and members of the Benfey lab for reviewing this manuscript. J.R.D. is supported by a Ruth Kirschstein National Research Service Award postdoctoral fellowship, T.A.L. by an NSF Minority Postdoctoral Research Fellowship, and S.M.B. by a Natural Sciences and Engineering Research Council postdoctoral fellowship. Funding to J.S. is provided by an NSF AT2010 grant (no. 0723493). This work was largely funded by an NSF AT2010 grant (no. 0618304) to P.N.B. The authors have declared that no competing interests exist. The National Center for Biotechnology Information Gene Expression Omnibus accession numbers for new microarray data discussed in this manuscript are GSE8787, GSE7642, GSE7641, GSE7639, GSE7636, and GSE10576.

Supporting Online Material

www.sciencemag.org/cgi/content/full/320/5878/942/DC1
 Materials and Methods
 SOM Text
 Figs. S1 to S13
 Tables S1 to S18
 References

5 December 2007; accepted 19 March 2008
 10.1126/science.1153795

ERRATUM

Post date 3 October 2008

Reports: "Cell identity mediates the response of *Arabidopsis* roots to abiotic stress" by J. R. Dinneny *et al.* (16 May, p. 942). On page 945, the URL for the supporting online material was incorrect. The correct URL is www.sciencemag.org/cgi/content/full/1153795/DC1.